Superexchange and electron correlations in alkali fullerides AC60, A = K, Rb, Cs

A. V. Nikolaev and K. H. Michel

Additional information on J. Chem. Phys.

Superexchange and electron correlations in alkali fullerides AC_{60}, A=K, Rb, Cs

A. V. Nikolaev[a)] and K. H. Michel
*Department of Physics, University of Antwerp, Campus Drie Eiken, Universiteitsplein 1,
2610 Antwerpen, Belgium*

Superexchange interactions in alkali fullerides AC_{60} are derived for C_{60} molecular ions separated by interstitial alkali-metal ions. We use a multiconfiguration approach which comprises the lowest molecular orbital states of the C_{60} molecule and the excited s and d states of the alkali-metal atom A. Interactions are described by the valence bond (Heitler–London) method for a complex $(C_{60}-A-C_{60})^-$ with two valence electrons. The electronic charge transfer between the alkali-metal atom and a neighboring C_{60} molecule is not complete. The occupation probability of excited d and s states of the alkali atom is not negligible. In correspondence with the relative positions of the C_{60} molecules and A atoms in the polymer crystal, we consider 180° and 90° (angle) superexchange pathways. For the former case the ground state is found to be a spin singlet separated from a triplet at $\sim$20 K. For $T<20$ K there appear strong spin correlations for the 180° superexchange pathway. The results are related to spin lattice relaxation experiments on CsC_{60} in the polymerized and in the quenched cubic phase. © *2005 American Institute of Physics*. [DOI: 10.1063/1.1844491]

I. INTRODUCTION

Superexchange,[1,2] i.e., the exchange coupling between relatively distant magnetic ions by the intermediary of normally diamagnetic ions, together with strong electron correlations,[3] plays a foremost role in determining the electron properties of a large class of *a priori* different materials. We mention the magnetic transition metal oxides,[2] the organic charge transfer salts,[4] the high T_c copper oxide superconductors,[5] and the molecule based magnets.[6] Strong electron correlations[7] are also found in a new class of organic conductors, the alkali-metal fullerides A_xC_{60}, where A is an alkali-metal atom and where C_{60} is the fullerene molecule.[8–10] The $x=3$ materials exhibit superconductivity,[11] while the $x=1$ compounds[12] form polymer phases.[13,14] At high temperature ($T \geqslant 350$ K) the $x=1$ compounds exhibit a plastic crystalline phase with cubic rocksalt structure (space group $Fm\bar{3}m$). NMR (Ref. 15) and electron spin resonance (ESR) (Ref. 16) experiments show that the electron spin susceptibility is of Curie type in the high T phase of AC_{60}. Upon slow cooling, stable polymer phases[13,14] of reduced symmetry are formed. The C_{60} molecules are linked through [2+2] cycloaddition and form chains along the former cubic [110] direction. The orientation of the polymer chains is characterized by the angle ϕ of the plane of cycloaddition with the former cubic [001] direction. The structure of KC_{60} is orthorhombic, space group $Pmnn$,[14] with alternating orientations $\pm\phi$ of the polymer chains in successive planes perpendicular to [001] and a same orientation of chains within a plane. The structure of both RbC_{60} and CsC_{60} is monoclinic,[17,18] space group $I2/m$. Here the polymer chains all have the same orientation ϕ. The lattice structure remains very close to orthorhombic. Parallel with the difference in structure, the electronic properties are different.[16] Polymerized KC_{60} is a 3D (three dimensional) metal which shows a metal-insulator phase transition combined with a structural phase transition near $T=50$ K.[19] On the other hand, RbC_{60} and CsC_{60} are considered as quasi–1D metals with antiferromagnetic fluctuations and 3D ordering of spin density waves below 50 K.[15,20]

The difference in structure and in electronic properties between KC_{60}, on one hand, and RbC_{60}, CsC_{60} on the other, suggests that the alkali-metal atoms have a specific role. This led us to the proposal of an alkali-mediated quadrupolar interaction between C_{60} molecular ions of different chains, where the driving mechanism is the partial occupation of excited electronic d states of the alkali-metal atoms.[21] This indirect interaction always favors the ferrorotational structure $I2/m$, while the direct interaction between chains favors the antiferrorotational structure $Pmnn$. The indirect alkali-mediated interactions are stronger in RbC_{60} and CsC_{60} than in KC_{60}.

In the present paper we study the alkali-mediated interaction between two C_{60} ions within a configuration interaction approach inspired by the concept of "interaction by indirect exchange" or superexchange.[2] Such an approach includes electron correlation effects which are beyond[22,23] the reach of conventional electronic band structure calculations. One remedy would be to include in the model the on-site Hubbard repulsion.[7] However, this procedure does not exhaust all correlation effects such as electron density fluctuations due to higher multipole Coulomb interactions.[24,25] These correlations are included in a method we have developed for the calculation of the valence electron and hole term scheme of the molecular ion $C_{60}^{m\pm}$, $m=2-5$.[24] The method is inspired by the theory of many

electron atomic states.[26] The present treatment of the $(C_{60}-A-C_{60})^-$ complex with two valence electrons requires as an extension the combination of the configuration interaction method with a Heitler–London approach of chemical bonding.[27]

The content of the paper is the following. Starting from the t_{1u} lowest unoccupied molecular orbitals (LUMO) of the C_{60} molecule and the electronic s and d states of the alkali-metal atom, we formulate the two valence electron basis states for the electronic configurations of the $(C_{60}-A-C_{60})^-$ complex (Sec. II). In the following (Sec. III) we use the Rayleigh–Ritz variational method to derive the secular resonance energy equation. Electron-electron Coulomb interactions are treated by multipole expansions. In Sec. IV we study the charge transfer between the central alkali-metal ion and the two surrounding fullerenes. We derive an expression for the alkali-metal Knight shift in AC_{60}. Next (Secs. V and VI) we calculate the superexchange energy spectrum of the complex for various bond orientations in the polymer phases $Pmnn$ and $I2/m$ and in the quenched cubic phase $Pa\bar{3}$. Electron spin correlations are investigated and compared with NMR experiments. Conclusions are formulated in Sec. VII.

II. CONFIGURATION INTERACTION

We construct the space of quantum states of the two valence electrons of the $(C_{60}-A-C_{60})^-$ molecular complex. Extending the Heitler–London treatment of the H_2 molecule, we retain $l=5$ LUMO states of the C_{60} molecules as well as excited s and d states of the alkali-metal atom.

The C_{60} molecule (240 valence electrons) is treated as a pseudoatom of icosahedral symmetry I_h.[24,28]

A. Single-particle states

The C_{60} molecule has the highest molecular point group I_h, where the parentage of π-molecular orbitals in spherical harmonics can be clearly traced.[8,29] Therefore, the type of irreducible representation (a, t_1, t_2, g, and h) and the orbital index l uniquely determine the angular dependence of the molecular orbitals. The angular functions are linear combinations of spherical harmonics adapted to the symmetry of the icosahedral group I_h.[30]

The t_{1u} LUMO corresponds to $l=5$ and has the following three angular components in Cohan's orientation, where the z axis is taken as one of the 12 fivefold axes of the C_{60} molecule and the y axis as one of the twofold axes perpendicular to z:[30,31]

$$\psi_1(t_{1u}) = \frac{6}{\sqrt{50}}Y_5^0 + \sqrt{\frac{7}{25}}Y_5^{5,c}, \tag{2.1a}$$

$$\psi_2(t_{1u}) = \sqrt{\frac{3}{10}}Y_5^{1,c} - \sqrt{\frac{7}{10}}Y_5^{4,c}, \tag{2.1b}$$

$$\psi_3(t_{1u}) = \sqrt{\frac{3}{10}}Y_5^{1,s} + \sqrt{\frac{7}{10}}Y_5^{4,s}. \tag{2.1c}$$

Here the normalized real spherical harmonics are defined with the phase convention of Ref. 32 [see also Appendix A,

Eqs. (A2a), (A2b), (A3a), and (A3b)]. In the following we start with the C_{60} molecule in the standard orientation of Ref. 33. If the C_{60} molecule is rotated by three Euler angles $\omega = (\alpha, \beta, \gamma)$ then the t_{1u} molecular orbitals are rotated too. The rotated orbitals are given by $\psi'_k = R(\omega)\psi_k$ ($k=1-3$), where $R(\omega)$ stands for the operator of the rotation. Knowing the transformation law for all $Y_{l=5}^\tau$ in Eqs. (2.1a), (2.1b), and (2.1c), one can find the expressions for ψ'_k.

The radial part $\mathcal{R}_t(r)$ is common for all t_{1u} orbitals. Here we use the radial part, which was deduced from a calculation of one carbon atom. It corresponds to model III of Ref. 24 and is discussed in Sec. V there.

The isolated alkali atom has only one s electron which is transferred to the fullerene molecule. (This is $4s$ for K, $5s$ for Rb, and $6s$ for Cs.) However, two things are important here. First, in a solid there is always a residual charge left at any alkali site and second, the crystal environment imposes a nonspherical perturbation so that mixing with some excited states with $l \neq 0$ should be taken into account.[21] Therefore, we consider a possibility for the transferred electron to occupy partly not only the s state but also one of the d states, which belong to the first excited shell above the s ground state level. The occupancy of excited d states is favored by the large interstitial space between polymer chains in the AC_{60} structure. The orbital part of the s state is Y_0^0, the orbital parts of the d shell are the five real spherical harmonics $Y_{l=2}^\tau$, where $\tau=0$, Eqs. (A2a), (A2b), (A3a), and (A3b). The radial parts are $\mathcal{R}_s(r)$ and $\mathcal{R}_d(r)$, respectively. They were obtained from atomic calculations (local density approximation) of K^+, Rb^+, and Cs^+. In total, there are six orbital functions for each alkali atom, which we label by the index $k^a = 1-6$.

Notice that here we do not assume *a priori* any particular occupation of s and d states. The populations will appear quite naturally as a result of our calculation.

B. Many electron basis states

The superexchange interaction operates through the excited states of the intermediate alkali atom, it implies a mixing of several electronic configurations.

The three electronic configurations which are relevant for our calculation are shown schematically in Fig. 1.

The first configuration (A) comprises two C_{60}^- monomers. Two electron basis ket vectors are given by

$$|I_A\rangle = |i_I^t, i_{II}^t\rangle. \tag{2.2}$$

The indices $i^t = (k, s_z)$ stand for the t_{1u} orbitals ($k=1,2,3$) and the spin projection. The wave functions are

$$\langle \vec{r}_1, \vec{r}_2 | I_A \rangle = \frac{1}{\sqrt{2}}(\langle \vec{r}_1 | i_I^t \rangle \langle \vec{r}_2 | i_{II}^t \rangle - \langle \vec{r}_1 | i_{II}^t \rangle \langle \vec{r}_2 | i_I^t \rangle), \tag{2.3}$$

where $\langle \vec{r} | i^t \rangle = \mathcal{R}_t(r) \langle \hat{n} | i^t \rangle$. Here $\mathcal{R}_t$ is the radial component of the t_{1u} molecular orbital, $\hat{n}$ stands for the polar angles $\Omega = (\Theta, \phi)$. There are six orientational t_{1u} vectors (or spin orbitals) $\langle \hat{n} | i^t \rangle$ (i.e., $i^t = 1-6$),

$$\langle \hat{n} | i^t \rangle = \psi_k(\hat{n}) u_s(s_z). \tag{2.4}$$

Here ψ_k are the three t_{1u} MOs as given by Eqs. (2.1a), (2.1b), and (2.1c) for Cohan's orientation of C_{60}, u_s is the spin func-
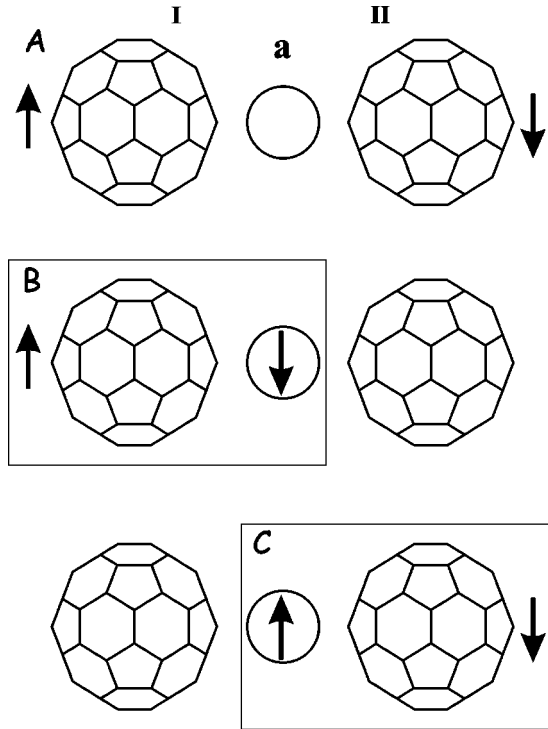
FIG. 1. Electronic configurations (A,B,C) for the superexchange: (A) $C_{60}^- - A^+ - C_{60}^-$; (B) $C_{60}^- - A - C_{60}$; (C) $C_{60} - A - C_{60}^-$. B and C are excited configurations where s and d states of the alkali atom are allowed. The transitions $A \leftrightarrow B$ and $A \leftrightarrow C$ involve the corresponding electron transfer from C_{60} to the alkali atom and back. The arrows $\uparrow$ or $\downarrow$ stand for the presence of an electron with spin, they do not imply a specific spin orientation.

tion $(s = \pm)$ for the spin projections $s_z = \pm 1/2$ on the z axis.

Each basis vector (2.2) corresponds to a 2×2 Slater determinant, Eq. (2.3), and the order of indices in Eq. (2.2) is important. As follows from the dynamical equivalence of the electrons the state $|i_{II}^t, i_I^t\rangle$ can be reduced to $|i_I^t, i_{II}^t\rangle$ by permuting the two electrons, i.e.,

$$|i_{II}^t, i_I^t\rangle = -|i_I^t, i_{II}^t\rangle. \tag{2.5}$$

To describe the same quantum state we will use the basis vectors (2.2) and apply the permutation law (2.5) when needed. Alternatively, one can use the corresponding Slater determinants for the two electron wave functions, Eq. (2.3). In total, we find $6 \times 6 = 36$ independent vectors, or determinants for the first configuration.

In order to describe the second configuration B, Fig. 1, we introduce the following basis ket vectors:

$$|I_B\rangle = |i_I^t, i_a\rangle, \tag{2.6}$$

where i_I^t labels the six spin orbitals of the C_{60}^- monomer and $i_a = (k^a, s_z)$ stands for 12 states of one electron on the alkali site. The orbital index k^a comprises either one s level or five orbital d states. The basis wave function is given by

$$\langle \vec{r}_1, \vec{r}_2 | I_B \rangle = \frac{1}{\sqrt{2}} (\langle \vec{r}_1 | i_I^t \rangle \langle \vec{r}_2 | i_a \rangle - \langle \vec{r}_1 | i_a \rangle \langle \vec{r}_2 | i_I^t \rangle). \tag{2.7}$$

The total number of basis states is $6 \times 12 = 72$.

Analogously, in the third electronic configuration, Fig. 1(C), the basis ket vectors are

$$|I_C\rangle = |i_{II}^t, i_a\rangle, \tag{2.8}$$

and the number of basis states is again 72.

We will operate in the quantum space of these three electronic configurations, with the total number of basis states $36 + 2 \times 72 = 180$. Notice that our quantum space is much larger than that in the traditional linear combination of atomic orbitals approach. The difference is accounted for by two electron correlations which are omitted in the conventional molecular orbital approximation. Our configuration space excludes states where the two electrons belong to a same C_{60} ion such as $|i_I^t, j_I^t\rangle$, $|i_{II}^t, j_{II}^t\rangle$, or to the alkali-metal ion such as $|i_a, j_a\rangle$. In this respect we consider a strongly correlated electron system in analogy with the Heitler–London theory.

Originally the idea of superexchange was applied to MnO.[2] There, is was assumed that the oxygen is in -2 state (O^{--}) so that its electronic shells are completely filled. Here we start with the alkali atom in the ionized state $+1$ (A^+), so that its electronic shells are also completely filled, although the charge of the mediator (i.e., an alkali atom) is positive in contrast with the negative charge of oxygen in MnO.

III. SECULAR PROBLEM

Starting from a Hamiltonian for $(C_{60} - A - C_{60})^-$ we formulate the secular problem in the configuration space (A, B, C) of Fig. 1. We take into account bond orientations depending on the relative positions of the alkali atom and the C_{60} molecules in the crystal.

The Hamiltonian for two valence electrons 1 and 2 (in atomic units) is

$$H = -\frac{1}{2}\nabla_1^2 - \frac{1}{2}\nabla_2^2 + \frac{1}{r_{12}} + V_{attr}^{C60}(r_1, r_2) + V_{attr}^a(r_1, r_2) + V_{cc}. \tag{3.1}$$

Here the first two terms describe the kinetic energy, while the third term represents the Coulomb repulsion between the electrons. $V_{attr}^{C60}(r_1, r_2)$ and $V_{attr}^a(r_1, r_2)$ stand for the attraction of the electrons to the fullerene molecules I and II and to the alkali atom, respectively:

$$V_{attr}^{C60}(r_1, r_2) = U^{C60(I)}(r_1) + U^{C60(I)}(r_2) + U^{C60(II)}(r_1)$$
$$+ U^{C60(II)}(r_2), \tag{3.2a}$$

$$V_{attr}^a(r_1, r_2) = U^a(r_1) + U^a(r_2). \tag{3.2b}$$

Notice that U^{C60} and U^a are single-electron potentials. Here U^{C60} refers to an effective attractive potential of the C_{60} molecule which includes the attractive potential of the carbon nuclei and the repulsive potential of the core states. As core states we consider all electronic shells except the valence t_{1u} level, because they are completely occupied and lie lower in energy. Here we consider U^{C60} being spherically symmetric. In our electronic system there are two molecules and therefore we consider two attractive potentials $U^{C60(I)}$ and $U^{C60(II)}$, respectively. Analogously, we introduce an effective attractive potential of the alkali atom U^a. We discuss the potentials U^{C60} and U^a in Appendix B. Finally, V_{cc} in Eq. (3.1) describes the repulsion between two C_{60} molecules and the

alkali atom. The calculation scheme for V_{cc} is also discussed in Appendix B.

Starting from the basis state vectors ($|I_A\rangle$, $|I_B\rangle$, $|I_C\rangle$) and the Hamiltonian (3.1), we use the Rayleigh–Ritz variational procedure to obtain the secular equation for the energy E:

$$|\hat{H} - E \cdot \hat{S}| = 0, \qquad (3.3)$$

where $\hat{H}$ and $\hat{S}$ are 180 by 180 matrices of Hamiltonian and overlap, correspondingly. As follows from the basis states the matrices $\hat{H}$ and $\hat{S}$ have a block form

$$\hat{H} = \begin{pmatrix} \hat{H}_{AA} & \hat{H}_{AB} & \hat{H}_{AC} \\ \hat{H}_{BA} & \hat{H}_{BB} & \hat{H}_{BC} \\ \hat{H}_{CA} & \hat{H}_{CB} & \hat{H}_{CC} \end{pmatrix}, \qquad (3.4)$$

with the submatrices $\hat{H}_{AA} = \langle I_A|H|J_A\rangle$, $\hat{H}_{AB} = \langle I_A|H|J_B\rangle$, etc. The submatrices AA, AB, etc., have dimensionality 36×36, 36×72, and so on. Notice also that $\hat{H}_{BA} = \hat{H}_{AB}^\dagger$, etc. The overlap matrix $\hat{S}$ has a similar structure with submatrices $\hat{S}_{AA} = \langle I_A|J_A\rangle$, $\hat{S}_{AB} = \langle I_A|J_B\rangle$, etc. Since we work in the basis with real spherical harmonics[32] our overlap matrix S is real and $S_{BA} = S_{AB}^T$, etc., where T stands for transpose.

A. Matrices of *A-A* block

We limit ourselves to the nearest neighbor approximation. This implies that there is no overlap between two electronic functions on two fullerenes, A, Fig. 1, i.e., $S_{AA} = \hat{1}$ and $H_{AA} = E_0 \cdot \hat{1}$, where $\hat{1}$ is the 36×36 unit matrix and $E_0 = 2E_{t1u}$. Here E_{t1u} is the one-electron energy of the valence electron on one C_{60}^- monomer. In the absence of superexchange the electronic states of two fullerene molecules are completely uncorrelated.

B. The technique of multipolar interaction: Application to the *B-B* block

The matrices of Hamiltonian H_{BB} and overlap S_{BB} belong to the *B-B* block, Eq. (3.4b). Since two electrons with overlap on different sites are involved, we distinguish direct and exchange terms:

$$\hat{S}_{BB} = \hat{S}_{BB}^{dir} + \hat{S}_{BB}^{exch}, \qquad (3.5)$$

where

$$\hat{S}_{BB}^{dir} = \delta(i_I^t, j_I^t)\delta(i_a, j_a), \qquad (3.6a)$$

$$\hat{S}_{BB}^{exch} = -s(i_I^t, j_a)s(i_a, j_I^t). \qquad (3.6b)$$

Here δ are Kronecker symbols and $s(i_a, j_I^t) = \langle i_a|j_I^t\rangle$ are the overlap matrix elements between alkali metal atom and fullerene molecule wave functions centered at different origins [see Eq. (B7)]. The same consideration applies to the configuration C, Fig. 1, and the *C-C* block.

We next consider the two particle interactions and will use a multipole expansion[24] of the Coulomb repulsion between two electrons (charge $e = -1$). The Coulomb potential between two electrons reads

$$V(\vec{r}, \vec{r}') = \frac{1}{|\vec{r} - \vec{r}'|}. \qquad (3.7)$$

The multipole expansion in terms of real spherical harmonics (Y_l^0, $Y_l^{m,c}$, and $Y_l^{m,s}$) is given by

$$V(\vec{r}, \vec{r}') = \sum_{l,\tau} v_l(r, r')Y_l^\tau(\hat{n})Y_l^\tau(\hat{n}'), \qquad (3.8)$$

where τ stands for $m = 0$, (m, c) or (m, s) of the real spherical harmonics and

$$v_l(r, r') = \left(\frac{r_<^l}{r_>^{(l+1)}}\right)\frac{4\pi}{2l+1}, \qquad (3.9)$$

with $r_> = \max(r, r')$, $r_< = \min(r, r')$.

Now we calculate the matrix element of the Coulomb repulsion for the electron transition $|i_I^t, i_a\rangle \rightarrow |j_I^t, j_a\rangle$. The direct Coulomb repulsion is obtained if we consider the $i_I^t \rightarrow j_I^t$ transitions for the first electron and the $i_a \rightarrow j_a$ transitions for the second. We call this transition "direct" transition after the Heitler–London model[27,34] which distinguishes direct and exchange integrals. In order to calculate the repulsion and make an advantage of the simple expression (3.9) we write the coordinate wave functions of C_{60} and the alkali at a same site, which can be either the first fullerene, Fig. 1, or the alkali atom. Details are given in Appendix A. Suppose we choose the fullerene site. Then we consider a set of alkali states $i_{a,p}$ projected from the initial alkali state i_a onto the first fullerene site. Each of the projected alkali states has its radial dependence $\mathcal{R}_{i_a,p}(r)$ which for simplicity we label by indices i_a and $p(q)$. Starting from Eq. (3.8) we obtain

$$\langle I_B|V(\vec{r}, \vec{r}')|J_B\rangle^{dir} = \sum_{l,\tau}\sum_{p,q} v_{p,q}^l \times c_{l,\tau}(i_I^t j_I^t)c_{l,\tau}(i_{a,p}j_{a,q}), \qquad (3.10)$$

where the transition matrix elements $c_{l,\tau}$ are defined by

$$c_{l,\tau}(ij) = \int d\Omega \langle i|\hat{n}\rangle Y_l^\tau(\hat{n})\langle\hat{n}|j\rangle. \qquad (3.11)$$

Here $\langle\hat{n}|j\rangle$ stands for the orbital part of the corresponding wave function. In case of C_{60} it is given by Eqs. (2.1a), (2.1b), and (2.1c). For $v_{p1,p2}^l$ in Eq. (3.10) we obtain

$$v_{p,q}^l = \int dr\, r^2 \int dr'\, r'^2 v_l(r, r') \\ \times \mathcal{R}_t^2(r)\mathcal{R}_{i_a,p}(r')\mathcal{R}_{j_a,q}(r'), \qquad (3.12)$$

where $\mathcal{R}_t(r)$ describes the radial dependence of the t_{1u} molecular orbitals. Extinction rules impose some restrictions on the values of l in Eq. (3.10). Indeed, since $l_{t1u} = 5$, Eqs. (2.1a), (2.1b), and (2.1c), from the theory of addition of angular momenta we know that $l_{min} = l_{t1u} - l_{t1u} = 0$ and $l_{max} = l_{t1u} + l_{t1u} = 10$. Furthermore, the odd values of l are excluded due to the parity of the integrand in Eq. (3.11). In the basis with the real t_{1u} orbitals, and with the real spherical harmonics Y_l^τ the coefficients $c_{l,\tau}$ are real.

The other possibility are the transitions $i_I^t \rightarrow j_a$ for the first electron and the transitions $i_a \rightarrow j_I^t$ for the second. This type of electron transition is called exchange[27,34] because the

C_{60} molecule and the alkali atom interchange their valence electrons. We use Eq. (2.5) to return to the standard order of the spin orbitals, and the parity is -1. As before, we project the alkali states i_a and j_a onto the states at the fullerene site. We find

$$\langle I_B|V(\vec{r},\vec{r}')|J_B\rangle^{exch} = -\sum_{l,\tau}\sum_{p,q} v'^l_{p,q} \times c_{l,\tau}(i^t_I j_{a,q}) c_{l,\tau}(i_{a,p} j^t_I), \tag{3.13}$$

where the coefficients $c_{l,\tau}$ again are given by Eq. (3.11), and $v'^l_{p,q}$ is found as

$$v'^l_{p,q} = \int dr\, r^2 \int dr'\, r'^2 v_l(r,r') \mathcal{R}_t(r) \mathcal{R}_{j_a,q}(r) \mathcal{R}_{i_a,p}(r') \mathcal{R}_t(r'). \tag{3.14}$$

The multipole index l here can be even or odd, the selection rules reduce the number of terms. The matrix element of the Coulomb repulsion of two electrons is found as

$$\langle I_B|V(\vec{r},\vec{r}')|J_B\rangle = \langle I_B|V(\vec{r},\vec{r}')|J_B\rangle^{dir} + \langle I_B|V(\vec{r},\vec{r}')|J_B\rangle^{exch}. \tag{3.15}$$

Analogously, we treat the single-particle interactions which include the kinetic energy and the effective attractive potentials (nucleus plus the core electrons). In general a single-electron operator $\mathcal{A}$ can be written as

$$\mathcal{A} = h(1) + h(2), \tag{3.16}$$

where h is the operator which acts only on the electron 1 or 2. For the direct transition we obtain

$$\langle I_B|\mathcal{A}|J_B\rangle^{dir} = \delta(i^t_I,j^t_I)\langle i_a|h|j_a\rangle + \langle i^t_I|h|j^t_I\rangle\delta(i_a,j_a), \tag{3.17}$$

where δ is the Kronecker symbol and $\langle i_a|h|j_a\rangle$ and $\langle i^t_I|h|j^t_I\rangle$ refer to the one-electron matrix elements which we describe in Appendix B. The exchange transition reads

$$\langle I_B|\mathcal{A}|J_B\rangle^{exch} = -s(i^t_I,j_a)\langle i_a|h|j^t_I\rangle - \langle i^t_I|h|j_a\rangle s(i_a,j^t_I), \tag{3.18}$$

where $s(i,j) = \langle i|j\rangle$ is the single-electron overlap matrix. In order to calculate the one-electron matrix elements of the type $\langle i_a|h|j^t_I\rangle$ where the wave functions belong to different sites, we also use the multipole expansion of the one particle quantity h and the technique of projection of states onto another site, see Appendix B. Finally, the matrix element $\langle I_B|\mathcal{A}|J_B\rangle$ is given by the sum of the contributions from Eqs. (3.17) and (3.18).

Using the expressions (3.17) and (3.18), we have calculated the overlap matrix $\langle I_B|J_B\rangle = S_{BB}$. Equations (3.17) and (3.18) can be applied to the spin-orbit coupling or to the interaction with external fields.

C. Couplings between *A* and *B*, and between *A* and *C* configurations

Here we find the matrix elements of the Hamiltonian $H_{AB} = \langle I_A|H|J_B\rangle$ and overlap $S_{AB} = \langle I_A|J_B\rangle$.

Since we limit ourselves by the nearest neighbor approximation we do not take into account the repulsion which refers to one electron located at the first fullerene molecule

and to the other electron which is delocalized between the alkali atom and the second C_{60} molecule, Fig. 1.

The single-particle part of the problem is dealt with as before. The coupling between the *A* states, $|i^t_I,i^t_{II}\rangle$, and *B* states, $|j^t_I,j_a\rangle$, is possible only for the transition $i^t_{II} \to j_a$ of the second electron while the first remains at the same site. We get

$$\langle I_A|\mathcal{A}|J_B\rangle = \delta(i^t_I,j^t_I)\langle i^t_{II}|h|j_a\rangle. \tag{3.19}$$

D. Coupling between *B* and *C* configurations

The coupling between the *B* states, $|i^t_I,i_a\rangle$, and the *C* states, $|j^t_{II},j_a\rangle$, occurs as a result of a two electron transfer: $i^t_I \to j_a$ and $i_a \to j^t_{II}$. The parity of the transition is -1, and as for the *A-B* and *B-C* cases we omit the two electron Coulomb repulsion because of the nearest neighbor approximation. For the one particle quantities $\mathcal{A}$ (overlap, kinetic energy, attractive pseudopotential) we find

$$\langle I_B|\mathcal{A}|J_C\rangle = -s(i^t_I,j_a)\langle i_a|h|j^t_{II}\rangle - \langle i^t_I|h|j_a\rangle s(i_a,j^t_{II}). \tag{3.20}$$

E. Bond orientation

The matrix elements are easily calculated if the center of mass of the C_{60} molecule and of the neighboring alkali-metal atom are located on a line parallel to the z axis. We call this situation a z bond. However, in general we have to consider a bond orientation described by the polar angles $\Omega = (\Theta, \phi)$. The corresponding $l=5$ h orbitals and the $l=2$ d orbitals have to be transformed by a rotation $R(\omega)$ according to the rules given for real spherical harmonics $Y^{m,c}_l$ and $Y^{m,s}_l$ in Appendix B of Ref. 24:

$$R(\omega)Y^\tau_l = \sum_{\tau'} Y^{\tau'}_l U^l_{\tau'\tau}(\omega), \tag{3.21}$$

where $\tau = (m,c)$, (m,s) and where ω stands for the Euler angles $\alpha = 0$, $\beta = \Theta$, $\gamma = \phi$. Here the rotator functions $U^l_{\tau'\tau}(\omega)$ are linear combinations of Wigner's D functions.[32]

We consider bond orientations and resulting superexchange pathways that correspond to the plastic phase (fcc lattice) or to the polymer phases of AC_{60} (orthorhombic lattice[14,17,18] for both *Pmnn* and *I2/m*) (Fig. 2).

In particular, we will consider the superexchange pathway $1-a_1-2$ where a_1-2 is a z bond and where $1-a_1$ is perpendicular to the z bond. We call this pathway a 90° superexchange. The pathway $1-a_2-3$ is called a 180° superexchange. With the help of Eq. (3.21) we transform the matrices computed for the z bond and obtain them for the bond with the polar angles Ω. The procedure for tensors with two indices is well known in the tight-binding method of Slater and Koster.[35] The transformation of one-electron matrix element of overlap reads

$$\langle Rl_1,\tau_1|Rl_2,\tau_2\rangle = \sum_{\tau',\tau''} U^{l_1}_{\tau'\tau_1}(\omega)U^{l_2}_{\tau''\tau_2}(\omega)\langle l_1,\tau'|l_2,\tau''\rangle. \tag{3.22}$$

The same law applies to all quantities which depend on two orbital indices. We also have some quantities which are
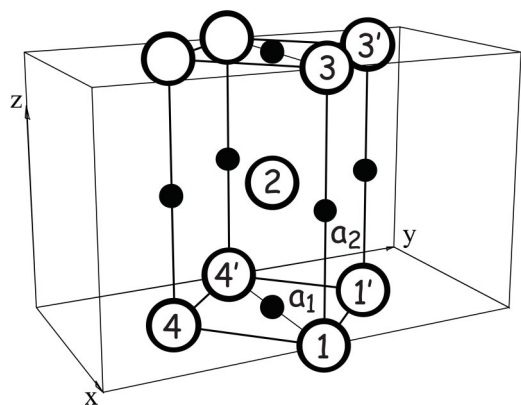
FIG. 2. Relation between the cubic and the orthorhombic unit cell in AC_{60}. Open circles stand for C_{60} molecules and full black circles for A atoms. Polymerization occurs along the $[1\bar{1}0]$ direction of the cubic system connecting $1-1'$ fullerene sites. The orthorhombic starting position of the C_{60} molecule requires a rotation by the angle $5\pi/4$ about the z axis.

given by four orbital indices. Those are transformed according to

$$\langle RI|V|RJ\rangle = \sum_{a,b,c,d} U^{l_1}_{a,\tau_1} U^{l_2}_{b,\tau_2} U^{l_3}_{c,\tau_3} U^{l_4}_{d,\tau_4} \langle I|V|J\rangle. \qquad (3.23)$$

Each bond geometry requires the complete solution of the secular problem.

IV. CHARGE TRANSFER

We present quantitative results obtained from the numerical solution of the secular problem, Eqs. (3.3) and (3.4).

In the limit of large distances $[d(C^{(I)}_{60}-A)=d(C^{(II)}_{60}-A) \to \infty]$ all overlap and transfer integrals become zero, and the ground state is characterized by uncorrelated electronic states of two electrons occupying t_{1u} molecular orbitals of two C_{60} molecules. The electron energy spectrum then consists of just three levels: (1) $2E_{t1u}-A$ configuration, (2) $E_{t1u}+E_s$, and finally, (3) $E_{t1u}+E_d$. The levels 2 and 3 correspond to the B and C configuration if the electron of the alkali atom is in a s or d state, respectively ($E_d > E_s$). Here E_{t1u} is the one-electron energy of the t_{1u} molecular orbitals of C_{60}, while E_s and E_d are the energies of the s and d states of the alkali atom. The position of the levels 1 and 2 is reversed if $E_s < E_{t1u}$. (In our calculations for Cs we find that $E_s=-5.3$ eV, while $E_d=-4.7$ eV.)

Here we treat E_{t1u} as a parameter, because in our approach the core states are not known accurately enough. We estimate E_{t1u} from photoelectron emission experiments by considering $E_{t1u}=\text{IP}-\Delta$, where IP is the ionization potential of the C_{60} molecule in the solid and where Δ is the highest occupied molecular orbital-LUMO energy separation. Taking IP ≈ -7.5 eV,[36] and $\Delta \approx -2.5$ eV (Ref. 37) we get $E_{t1u} \approx -5$ eV. This energy is in the region where one expects the hybridization with the s and d states of Cs. Our calculations support this viewpoint, see Fig. 3. In our calculations the distance between C_{60} and Cs was taken from the cubic phase, i.e., $d(C_{60}-\text{Cs})=7.065$ Å.

In order to analyze the results we have calculated three occupation probabilities or statistical weights: $P[C_{60}-C_{60}]$ for finding two electrons on each molecule, $P[C_{60}-\text{Cs}(s)]$
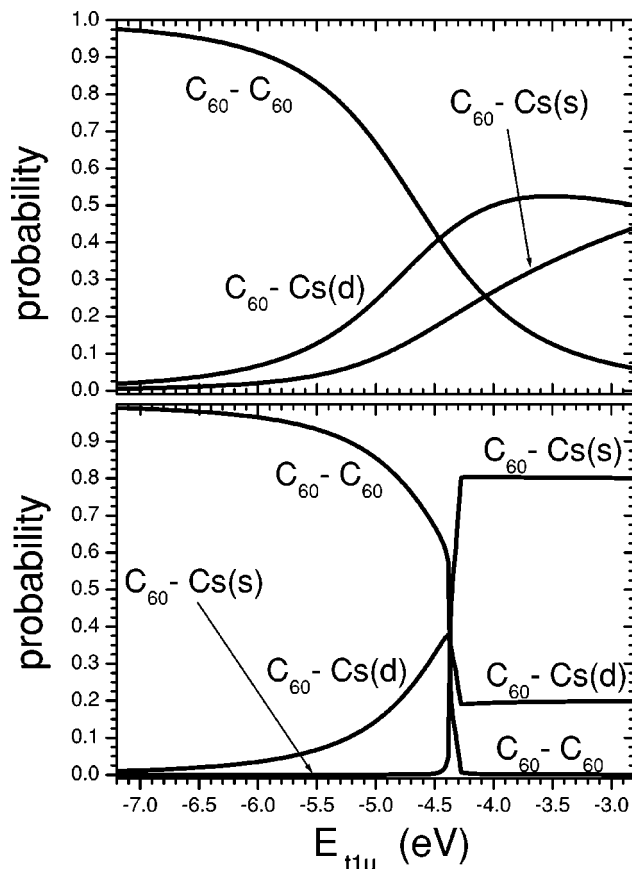

FIG. 3. Probabilities of configurations: (1) Two electrons occupy two fullerene molecules $[C_{60}-C_{60}]$; (2) one of the electrons occupies one of the C_{60} molecules while the second one is in the s state of Cs $[C_{60}-\text{Cs}(s)]$; (3) one of the electrons occupies one of the C_{60} molecules while the second is in one of the d state of Cs $[C_{60}-\text{Cs}(d)]$. Upper panel: 90° superexchange $1-a_1-2$. Lower panel: 180° superexchange $1-a_2-3$. The C_{60} molecules are in standard orientation.

for one electron on C_{60} and the other in the s state of Cs, and $P[C_{60}-\text{Cs}(d)]$ for one electron on C_{60} and the other in the d states of Cs. These occupation probabilities are calculated by using the components corresponding to the configurations A, B, C, respectively, of the 180-dimensional eigenvector of the ground state. For the case of 90° superexchange geometry, upper panel of Fig. 3, we find that for $E_{t1u}=-5$ eV there is still a significant weight of s and d states of Cs: $P[C_{60}-\text{Cs}(s)]=0.089$ and $P[C_{60}-\text{Cs}(d)]=0.244$. The probability $P(C_{60})$ to find an electron on the t_{1u} level is calculated as

$$P(C_{60}) = P[C_{60}-C_{60}] + \frac{1}{2}[P[C_{60}-\text{Cs}(s)] + P[C_{60}-\text{Cs}(d)]] = 0.834. \qquad (4.1)$$

This result has to be confronted with the commonly accepted opinion that the charge transfer from the alkali-metal atom to the LUMO states of the C_{60} molecule is almost complete.[7–10] However, there are many reservations in respect to this conclusion coming from first principles calculations. For example, Andreoni et al.[38] have found that if the crystal space is divided into Voronoy polyhedra (i.e., Wigner–Seitz-like cells), then the integrals on the cells give the charge $0.2-0.3e$ for potassium sites in K_3C_{60} (Table III of Ref. 38). The same conclusion has followed from the calculation of AC_{60} ($A=$ K, Rb, Cs) of Jorissen and Lamoen,[39]

who used Bader's partition[40] of crystal space. Their calculation indicates that a large portion of charge $(0.1–0.15\ e)$ is located close to the alkali atom and is aspherical in agreement with our idea of partial occupancy of d orbitals. This conclusion is not unexpected in connection with incomplete charge transfer $(0.7\ e)$ found in alkali graphite intercalation compounds.[41] On the other hand, the common opinion on the charge transfer is drawn from NMR Knight shift experiments[15] where the shift at the alkali-metal atom line is very small. The experiments of Tycko *et al.*[15] demonstrate an increase of the Knight shift with decreasing temperature in the high T cubic phase of AC_{60}. For a theoretical explanation, Tycko *et al.* consider the excess electrons as primary localized on C_{60}^- ions where they act as quasifree paramagnetic centers. Replacing then the Pauli spin susceptibility by a Curie law type susceptibility for free electrons, Tycko *et al.* give a well founded explanation of the temperature dependence of the measured Knight shift. Their view of paramagnetic electrons on the C_{60}^- ions has been corroborated later by ESR measurements of the electron spin susceptibility.[16] We now show that within the frame of the present theory a small value of the measured Knight shift can be understood. Within the standard theory, the Knight shift due to Fermi contact coupling is given by[42]

$$K = \frac{\Delta \nu_0}{\nu_0} = \frac{8\pi}{3}\langle |\psi_s^a(0)|^2\rangle \chi_e. \qquad (4.2)$$

Here $\langle |\psi_s^a(0)|^2\rangle$ is an average over the squared s wave function, taken at the position of the alkali nucleus, χ_e is the Pauli susceptibility. In a first step we follow Tycko *et al.*[15] and replace χ_e by the paramagnetic electronic susceptibility χ_{para}.

$$\chi_{para} = \frac{1}{4}\frac{\gamma_e^2\hbar^2 N_e}{k_B T}, \qquad (4.3)$$

where γ_e is the magnetogyric ratio of the electron and N_e the number of paramagnetic electrons per unit volume. In a second step we notice that the paramagnetic spin density at the alkali-metal nucleus is due to the t_{1u} electron localized on the C_{60} molecule. Hence we have to calculate the overlap of the s wave function, centered at the alkali nucleus with the t_{1u} wave function centered on the molecule:

$$\langle i_a^{(s)}, j_I^t\rangle = s(i_a^{(s)}, j_I^t). \qquad (4.4)$$

The overlap matrix element s has been introduced in Eq. (3.6b). Numerical evaluation by means of Eq. (B7) gives $s(i_a^{(s)},j_I^t)=0.0326$ and 0.0348 for CsC_{60} and KC_{60}, respectively. Account of this overlap leads to a reduction of $\langle|\psi_s^a(0)|^2\rangle$ by a factor $s^2(i_a^{(s)},j_I^t)$. Furthermore, we take into account the probability $p(C_{60})\approx 0.834$ to find one electron on C_{60} and notice that there are six C_{60} molecules around the alkali-metal atom. We then obtain the expression

$$K = 16\pi P(C_{60})s^2(i_a^{(s)},j_I^t)\langle|\psi_s^a(0)|^2\rangle\chi_{para} \qquad (4.5)$$

for the Knight shift. We see that the factor $s^2(i_a^{(s)},j_I^t)\sim 10^{-3}$ leads to a major reduction of the Knight shift. We conclude that the small experimental value of the Knight shift does not imply an almost complete charge transfer for s electrons.
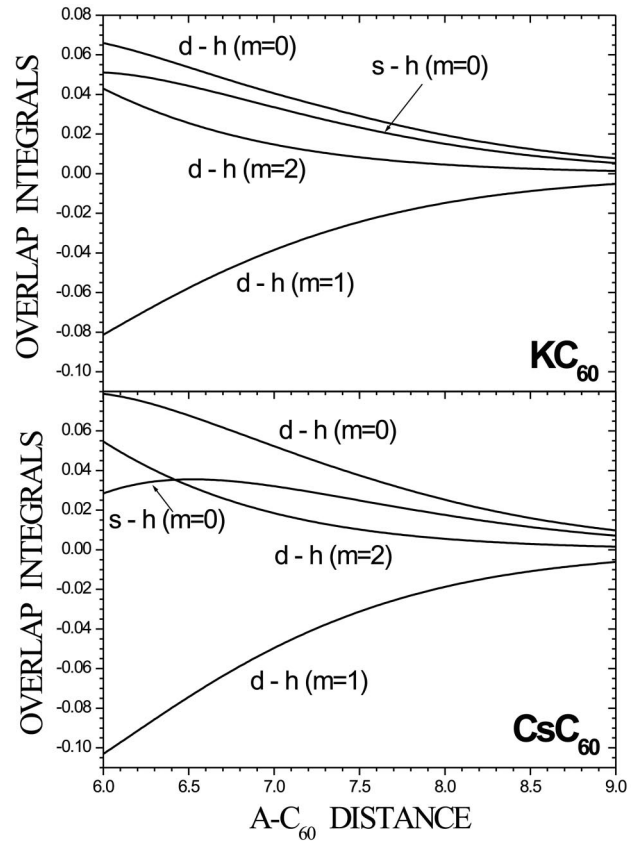

FIG. 4. Overlap integrals between s or d states of the alkali atom (K or Cs) and the h manifold (11 functions $Y_{l=5}^\tau$ with $l=5$) representing the orbital part of t_{1u} molecular orbitals. Only integrals with the same azimuthal dependence τ [(m,c) or (m,s)] are not zero. Distance is in ångströms (Å).

The present theory [see Eq. (4.1)] gives a non negligible occupancy for s electrons and even a higher occupancy for d electrons at the alkali nucleus site. In order to understand this fact we calculated the overlap integrals between C_{60} and the alkali atom in positions $1-a_2$, Fig. 2. The overlap was computed between s and d states and the 11 h states with the orbital index $l=5$ (real spherical harmonics Y_5^τ with the radial dependence for the C_{60} LUMO). The results for CsC_{60} are shown in Fig. 4.

There is an important selection rule here: only the integrals between orbitals with the same azimuthal dependence (ϕ) are not zero. By inspecting the orbital parts of t_{1u} functions, Eqs. (2.1a), (2.1b), and (2.1c), we conclude that the s state of Cs can only couple with the first function $\psi_1(t_{1u})$ containing Y_5^0, while the d states hybridize with all three orbitals $\psi_k(t_{1u})$, $k=1-3$. Therefore, mixing with d states gives more variational degrees of freedom and explains the fact that $P[C_{60}-Cs(d)]>P[C_{60}-Cs(s)]$. The overlap with d states is larger for Cs than for K. This fact corroborates our hypothesis[21] about the decisive role of d states mediated interactions between C_{60} chains in competition with the direct interactions.

All these findings refer to the regime where E_{t1u} <-4.4 eV. At higher energies the behavior of superexchange changes drastically, especially for the 180° superexchange, Fig. 3, lower panel. Increasing E_{t1u} we observe that at ~-4.4 eV $P[C_{60}-C_{60}]$ abruptly changes to zero. This im-
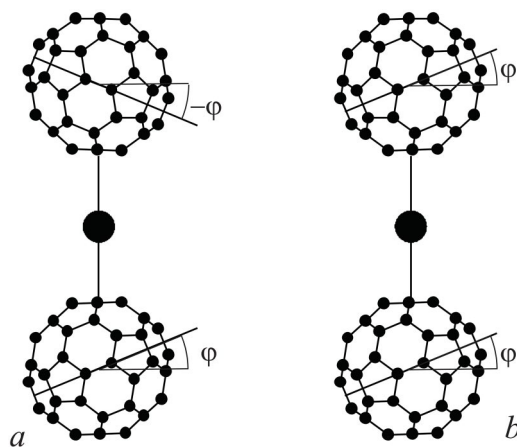
FIG. 5. Antiferro- and ferro-orientations of two fullerene molecules with 180° superexchange: (a) $\varphi_2 = -\varphi_1$, (b) $\varphi_2 = \varphi_1$.

plies that the electronic system resonates between configurations B and C, Fig. 1. In this regime the weight of s states is larger than the weight of d states. The 90° superexchange, Fig. 3 (upper panel), also undergoes a transition to this regime but in a continuous way. This region of our calculations is unrealistic because it corresponds to the situation when the alkali atom acts as an electron acceptor by retaining its electron in the crystal. In the following we discard the resonating regime and put $E_{t1u} = -5$ eV.

V. POLYMER PHASES

A. Superexchange interactions

The polymerization and transition to the orthorhombic lattice occur below about 350 K. In fact, the low temperature phase of RbC_{60} and CsC_{60} is monoclinic ($I2/m$) but the deviation from the orthorhombic symmetry is very small.[17,18] The polymerization takes place along one of the former cubic [110] directions. In Fig. 2 the polymer chains connect the fullerene molecule 1 and $1'$, 3 and $3'$, 4 and $4'$, etc. (the $[1\bar{1}0]$ cubic direction).

As a superexchange complex we can choose the fullerene molecules 1 and 2 with the alkali atom at site a_1 or a_2. We label these complexes as $1-a_1-2$ and $1-a_2-2$, respectively. Among other possibilities we consider complexes $1-a_2-3$, $1-a_1-4'$, and $1-a_1-4$. In general they have different energies of the ground state. We have studied their energy spectrum as a function of molecular orientation. For two C_{60} molecule we considered antiferro- and ferro-orientations as shown in Fig. 5 [cases (a) and (b), respectively].

The molecular starting orientation is such that one of its twofold axis coincides with the twofold cubic axis (i.e., $[1\bar{1}0]$ axis). The starting position is obtained from the standard orientation of the cubic phase[33] through a rotation by $5\pi/4$ about the z axis.[28] Therefore, the starting position in the orthorhombic phase *differs* from the standard orientation of C_{60} in the cubic crystal. We then rotate the molecules by an angle ϕ about the twofold axis (cubic $[1\bar{1}0]$ axis) which is also the direction of polymerization. The results for the ferro-rotations are shown in Fig. 6.
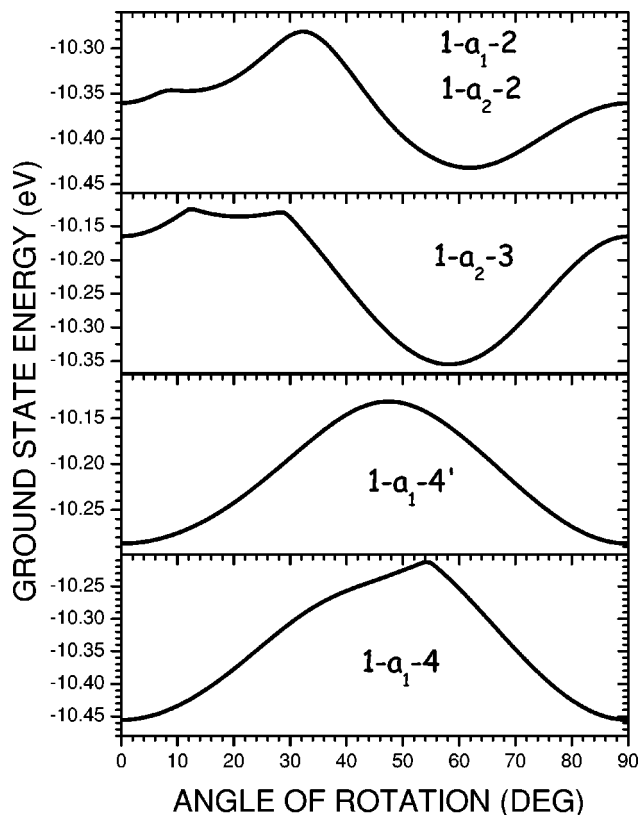

FIG. 6. The energy of the ground state as a function of rotation of two fullerene molecules, $\varphi_2 = \varphi_1$. Each plot corresponds to different superexchange pathways as shown in Fig. 2.

As one can see the ground state energy strongly depends on the angle of rotation. The 90° superexchange complexes for the $1-a_1-2$ and $1-a_2-2$ pathways give the same results as is also obvious from symmetry. In general, different pathways lead to different results and sometimes competing interactions.

One of our motivations for the study of superexchange interaction was to understand the difference between antiferro- and ferro-orientations of the polymer chains.[14,17] The first is realized for KC_{60}, the second for RbC_{60} (Ref. 17) and CsC_{60}.[18] The important pathway then is $1-a_1-2$. In Table I we have quoted part of the energy spectrum obtained

TABLE I. Energy spectrum of antiferro-($\varphi_2 = -\varphi_1 = 45°$) and ferro-($\varphi_2 = \varphi_1 = 45°$) orientations of two fullerene molecules. The 90° superexchange pathway is $1-a_1-2$ or $1-a_2-2$, $E_{t1u} = -5$ eV. The triple degeneracy corresponds to spin components $S_z = \pm 1, 0$, the single to $S_z = 0$.

$\varphi_2 = -\varphi_1 = 45°$		$\varphi_2 = \varphi_1 = 45°$	
E (eV) (deg)	$E - E_{gs}$ (K)	E (eV) (deg)	$E - E_{gs}$ (K)
−10.361 89 (3)	0	−10.362 19 (3)	0
−10.361 68 (1)	2.4	−10.362 00 (1)	2.2
−10.335 22 (1)	309.5	−10.334 22 (3)	324.6
−10.334 99 (3)	312.2	−10.334 08 (1)	326.2
−10.297 07 (3)	752.2	−10.297 46 (1)	751.2
−10.297 05 (1)	752.4	−10.297 11 (3)	755.2
...	...	...	...
−8.769 82 (3)	18 475.2	−8.770 74 (3)	18 468.0

TABLE II. Energy spectrum of antiferro-($\varphi_2=-\varphi_1=45°$) and ferro-($\varphi_2=\varphi_1=45°$) orientations of two fullerene molecules. The 180° superexchange pathway is $1-a_2-3$, $E_{t1u}=-5$ eV.

$\varphi_2=-\varphi_1=45°$		$\varphi_2=\varphi_1=45°$	
E (eV) (deg)	$E-E_{gs}$ (K)	E (eV) (deg)	$E-E_{gs}$ (K)
−10.289 40 (3)	0	−10.286 86 (1)	0
−10.287 95 (1)	16.8	−10.283 15 (3)	43.1
−10.206 12 (1)	966.4	−10.208 49 (3)	909.4
−10.205 80 (3)	970.1	−10.207 63 (1)	919.4
−10.204 93 (1)	980.2	−10.205 72 (3)	941.6
…	…	…	…
−8.504 36 (3)	20 714.5	−8.491 61 (3)	20 833.0

TABLE III. Ground state and first excited states for different superexchange pathways of the orthorhombic structure. F stands for ferro-($\varphi_2=\varphi_1=45°$) and A for antiferro-($\varphi_2=-\varphi_1=45°$) orientations of two molecules.

Superexchange pathway	$C_{60}-C_{60}$ orientation	Ground state	First excited state	Gap (K)
$1-a_1-2$	F	Triplet	Singlet	2.2
$1-a_1-2$	A	Triplet	Singlet	2.4
$1-a_2-3$	F	Singlet	Triplet	43.1
$1-a_1-4$	F	Triplet	Singlet	0.5
$1-a_1-4'$	F	Singlet	Triplet	20.2
$1-a_1-1'$	F	Singlet	Triplet	0.5

from the solution of the secular problem. From the lowest energy levels we see that the ferrorotational orientation between two C_{60} molecules 1 and 2 around the alkali-metal atom a_1 is only by ~3.3 K lower in energy than the antiferrorotational orientation. Notice however that the alkali-metal atom a_1 is traversed by eight equivalent 90° superexchange pathways which favor the ferrorotational structure. The ferrorotational interaction mediated by the excited d states of the alkali-metal atom a_1 can be regarded as the product of two electric quadrupole-quadrupole interactions of the alkali-metal atom with the two surrounding C_{60} molecules 1 and 2.[21] Our calculations are based on the t_{1u} LUMO states of the structurally undeformed C_{60} molecule. The corresponding quadrupole moment has been calculated in Ref. 43. Recently, it has been shown[44] that the electric quadrupole moment of the deformed C_{60}^- monomer in the polymer chain is substantially larger than for the undeformed molecular ion. Hence we expect that in the real crystal the superexchange interaction is larger than for the idealized complex $(C_{60}-A-C_{60})^-$. In any case the superexchange effect is quite substantial.

The energy gain of the ground state $E_{gs}-2E_{t1u}$ is ~0.4 eV and the overall energy splitting is ~1.5 eV.

In fact, the effect of superexchange here is inseparable from the phenomenon of chemical bonding. In Table II we have given the energy spectrum for a 180 superexchange pathway.

B. Low temperature spin correlations of the polymer phase of CsC$_{60}$

The important feature is the existence of low lying excited states. Depending on the orientations of two molecules and the position of the alkali atom, the ground state is either a triplet or a singlet. The triplet state is magnetic. Its contribution to the magnetic susceptibility is of Curie type. In the singlet state the contribution to the magnetic susceptibility is temperature independent (van Vleck paramagnetism). If the ground state is singlet (nonmagnetic) then the first excited state is triplet (magnetic) and vice versa. The energy gap between ground state and first excited state becomes crucial at low temperatures. Both the ground state and the gap are very sensitive to the molecular orientations and the alkali position, as summarized in Table III.

From Table III we also notice that for a number of cases

$(1-a_1-2, 1-a_1-4, 1-a_1-1')$ the gap is extremely small. If there is no energy difference between a singlet and triplet states, the two electron spins are independent. This implies that there are no spin correlations due to superexchange between two electrons on the fullerene molecules 1 and 2, or 1 and 4, or 1 and 1'. Notice that all these cases are 90° superexchange pathways, and that 1 and 1' are intrachain neighboring sites.

In the 180° interchain pathways $1-a_2-3$ and $1-a_1-4'$ the gap is much larger. The first excited state for these cases is a triplet, while the ground state is a singlet. Characteristic temperatures are $T_s\sim20$ K and ~43 K. At high temperatures $(T>T_s)$ the triplet level is populated and contributes to the susceptibility according to the Curie law. Upon cooling below T_s, a spin gap becomes effective, imposing spin correlations for electrons on fullerenes 1 and 3 or 1 and 4' located on different polymer chains. It is tempting to relate these theoretical results to NMR experiments[45,46] in polymerized CsC$_{60}$ where a transition to a nonmagnetic spin singlet state takes place at $T_s\approx13.8$ K.

We conclude that the singlet ground state binds electron spins on different chains through 180° superexchange. The spins of electrons at 90° superexchange are almost free. Therefore, we expect a correlated state of electron spins at fullerene site sequences $4'-1-3-\ldots$ or $4-1'-3'-\ldots$ and so on, with weak or no correlations between those series. Synchrotron x-ray powder diffraction experiments[18] reveal that a spontaneous strain appears along both the polymer chain axis and the interchain orthorhombic [111] direction below the spin singlet transition temperature T_s.

VI. CUBIC ORDERED CsC$_{60}$

By quenching CsC$_{60}$ in the cubic plastic phase ($Fm\bar{3}m$) from $T>350$ K to liquid nitrogen temperature, a metastable cubic ordered phase, also called quenched cubic phase, is obtained,[47] with space group $Pa\bar{3}$. (Notice that the same space group is realized in the orientationally ordered phase below $T_c\approx255$ K in pristine C_{60}.[33,48,49]) The $Pa\bar{3}$ structure is simple cubic and it has four different sublattices n_1-n_4, which contain the sites $(0,0,0)$, $a/2(0,1,1)$, $a/2(1,0,1)$, and $a/2(1,1,0)$, respectively. The sublattices differ by molecular orientations. The molecular threefold axes lie along the four main cube diagonals: $[111]$, $[\bar{1}\bar{1}1]$, $[1\bar{1}\bar{1}]$, and $[\bar{1}1\bar{1}]$ for n_1, n_2, n_3, and n_4, correspondingly. The molecules can be rotated simultaneously by a setting angle ϕ away from the standard
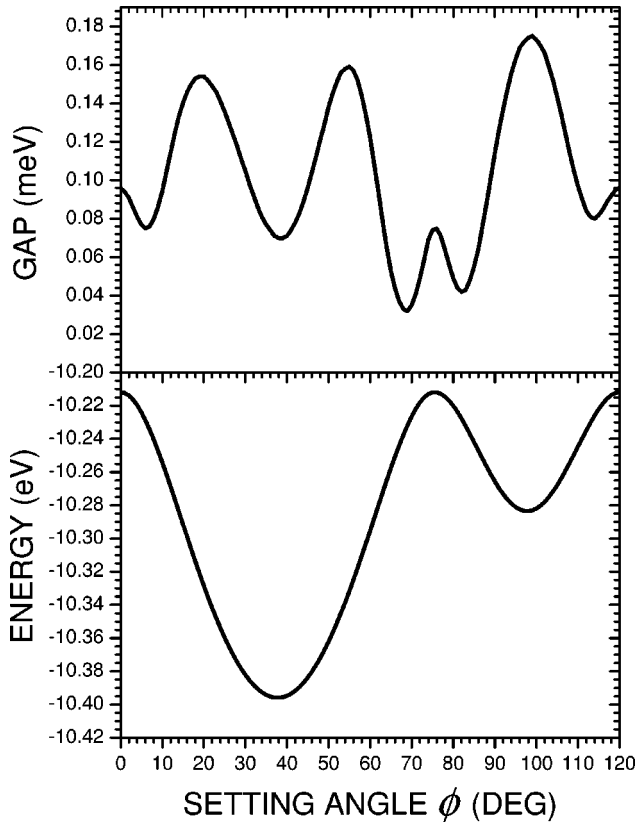
FIG. 7. Lower panel: Superexchange energy of the ground state (triplet) as a function of simultaneous rotation by an angle ϕ of two fullerene molecules in the cubic ordered phase. The pathway is $1-a_1-2$ or $1-a_2-2$, Fig. 2. The two C_{60} molecules belong to two different sublattices. Upper panel: Energy gap between the ground state (triplet) and the first excited state (singlet).

TABLE IV. Energy spectrum for the 90° superexchange pathway $1-a_1-2$ or $1-a_2-2$. The setting angles ϕ_1 and ϕ_2 correspond to two competing minima of the C_{60} ordered phase.

$\phi_1=38°$		$\phi_2=98°$	
E (eV) (deg)	$E-E_{gs}$ (K)	E (eV) (deg)	$E-E_{gs}$ (K)
−10.395 91(3)	0	−10.283 49(3)	0
−10.395 84(1)	0.8	−10.283 32(1)	1.97
−10.287 40(1)	1259.2	−10.238 04(1)	527.4
−10.287 31(3)	1260.2	−10.237 98(3)	528.1
−10.286 33(3)	1271.6	−10.237 18(3)	537.4
−10.286 18(1)	1273.4	−10.237 04(1)	539.0
…	…	…	…
−8.779 72(1)	18 755.1	−8.789 57(1)	17 336.2

triplet, Fig. 7 and Table IV. As a result the electron spins of fullerenes 1 and 2 are almost independent at temperatures $T>1\ K$.

However, the electron spin correlation are enabled by the 180° superexchange $(1-a_2-3)$ which connects two C_{60} molecules belonging to the same sublattice n_i $(i=1-4)$. The characteristic temperature here is $T_s\sim 22$ or $39\ K$, Table V. At temperatures $T>T_s$ spins are uncorrelated. The thermal occupation of the triplet state gives a Curie contribution to the magnetic susceptibility. At low temperatures $T<T_s$ the spin gap sets in which accounts for the singlet ground state and a decrease of the magnetic susceptibility. ^{13}C NMR spin lattice relaxation experiments in quenched CsC_{60} show for $T<50\ K$ the partial opening of a spin gap[51,52] which indicates a deviation from metallic behavior. ^{133}Cs NMR spectra[51,52] indicate the existence of localized spin singlets. While in Ref. 52 it is suggested that the spin singlets are localized on the C_{60} balls (i.e., C_{60}^{2-}), we rather suggest that the spin singlets are localized on the $(C_{60}-A-C_{60})^-$ complexes as a consequence of superexchange. The latter mechanism avoids the need to overcome the strong onsite Coulomb repulsion. We notice that each Cs site in the $Pa\bar{3}$ structure is traversed by three possible 180° superexchange pathways and hence a random distribution of singlet carrying $(C_{60}-A-C_{60})^-$ complexes in the CsC_{60} crystal becomes possible.

orientation in the following way: those which belong to n_1 are rotated about the $[111]$ cubic axis, the molecules which belong to n_2 about the $[\bar{1}\bar{1}1]$ cubic axis, etc. In pristine C_{60} the crystal energy exhibits two minima as a function of the setting angle ϕ: a primary minimum at $\phi_1=98°$ and a secondary one at $\phi_2=38°$.[33,50] The quenched cubic phase of CsC_{60} arose special interest[51,52] because it is metallic[47] without formation of the polymer chains. We have solved the superexchange problem for two neighboring C_{60} molecules in the $Pa\bar{3}$ phase of CsC_{60}. In Fig. 7 we show the energy as a function of the setting angle ϕ for various pathways. The starting position of the molecule before rotation by ϕ is now the standard orientation.[33]

The pathway $1-a_1-2$, referring to the energy plot in Fig. 7 connects two fullerene molecules belonging to the sublattices n_1 and n_2. The same plot is obtained for two molecules belonging to other sublattices: n_1 and n_3, and n_1 and n_4, as anticipated from the symmetry.

The calculated energy spectra for the $1-a_1-2$ and $1-a_2-3$ superexchange pathways are quoted in Tables IV and V. The superexchange binding energy is ~0.3 eV and the total span of energy levels is ~1.5 eV.

The 90° superexchange which connects two fullerene molecules belonging to different sublattices, for example n_1 and n_2 $(1-a_1-2$ or $1-a_2-2)$, leads to a triplet ground state. The first excited states is singlet which lies very close to the

TABLE V. Energy spectrum for the 180° superexchange pathway $1-a_2-3$. The ground state is singlet, the first excited state is triplet. The angles ϕ_1 and ϕ_2 correspond to two competing minima of the C_{60} ordered phase.

$\phi_1=38°$		$\phi_2=98°$	
E (eV) (deg)	$E-E_{gs}$ (K)	E (eV) (deg)	$E-E_{gs}$ (K)
−10.25 009(1)	0	−10.173 45(1)	0
−10.24 673(3)	39.0	−10.171 51(3)	22.5
−10.18 075(3)	804.7	−10.149 61(1)	276.7
−10.18 052(1)	807.3	−10.148 88(3)	285.1
−10.17 895(3)	825.5	−10.147 92(3)	296.3
−10.17 688(1)	849.6	−10.145 47(1)	324.7
…	…	…	…
−8.57 906(3)	193 914.7	−8.695 03(3)	17 156.3

From our theoretical study of the low temperature cubic phase of CsC_{60} emerges the picture of a singlet ground state for any pair of C_{60} molecules belonging to the same sublattice and no spin correlations between C_{60} molecules from different sublattices. Anomalies may be present at $T \sim 1$ K because of correlations between electron spins from different sublattices.

VII. CONCLUSIONS

We have presented a systematic configuration interaction study of the superexchange mechanism in a $(C_{60}-A-C_{60})^-$ complex where A is an alkali-metal atom (ion). We have investigated the resonance energy problem[27] with two valence electrons as a function of the positions of the A atom and the C_{60} molecules (superexchange bond geometry) and as a function of molecular orientations. The method is appropriate to investigate superexchange in various phases of the AC_{60} compounds: high temperature plastic phase with orientational disorder (space group $Fm\bar{3}m$), polymer phases for $T < 350$ K with space group $Pmnn$ in KC_{60} and $I2/m$ in RbC_{60}, CsC_{60}, quenched cubic phase with space group $Pa\bar{3}$ in CsC_{60}. By solving the secular equation we obtain the energy spectrum and the corresponding wave functions. We then find (Sec. IV) that due to superexchange the charge transfer between the alkali-metal atoms and C_{60} molecules is not complete. There is a significant weight for excited electronic s and d states on the alkali-metal atom. In particular, the probability of finding one electron on C_{60} and the other in the d state of the neighboring Cs is 0.224. This effect is larger for Cs and Rb than for K. The relatively large value (0.089) of the probability of finding one electron on C_{60} and the other in the s state of the alkali is not at variance with NMR Knight shift results on ^{87}Rb and ^{133}Cs in AC_{60}. We have derived a theoretical expression for the Knight shift, taking into account the overlap between electronic s wave functions centered at alkali-metal atom and t_{1u} wave functions centered on the C_{60} molecule. The small value of the experimental Knight shift is compatible with our theoretical results of rather incomplete charge transfer.

The theory provides an information on electron spin correlations. Below $T \approx 20$ K, we find the opening of a spin gap in polymerized CsC_{60} (Sec. V) where the singlet ground state binds electron spins on different chains through 180° superexchange. We relate these results to NMR experiments[45,46] in polymerized CsC_{60}. We have applied the theory to the quenched $Pa\bar{3}$ phase of CsC_{60}. We find that at T below 20 K a spin gap sets in which accounts for the singlet ground state. Spin correlations occur due to 180° superexchange between neighboring C_{60} molecules on a same simple cubic sublattice of the $Pa\bar{3}$ structure. There are no spin correlations between different sublattices. Experimental evidence for localized spin singlets has been given by NMR experiments.[51,52]

The present method allows to calculate superexchange spin correlations and chemical bonding. It combines the configuration interaction (CI) approach with the valence bond[27] (VB) treatment. In fact, that the CI is an essential part of superexchange was realized by Keffer and Oguchi.[53] Superexchange cannot be described in the framework of electron

band structure calculation. The second ingredient of the present theory, VB treatment, is generically a many electron approximation[54] involving many electron determinants. The VB method yields automatically the desired atomic electron term splittings, which is not the case for the molecular orbital method. The combination of the VB treatment with the CI approach allows us to construct and to solve the secular equation from first principles rather than to use perturbation theory. In the present paper we deal with two valence electrons, but the treatment can be easily generalized for a larger number of electrons. Then one has to take into account the Coulomb multipole interactions on the same site which gives rise to atomic electron term structure and Hund rules.

While the present work has been motivated by our interest in the alkali-metal fullerides A_1C_{60}, our approach to the problem of superexchange is suitable for application to other materials. As example we mention d and f elements,[55] i.e., transition metals and lanthanides or actinides, respectively. Our method should be useful for the description of strongly correlated electrons in other alkali fullerides[10] such as A_3C_{60} and in high T_c superconductors.[3,5,56]

ACKNOWLEDGMENTS

APPENDIX A: EXPANSION OF A COORDINATE WAVE FUNCTION AT ANOTHER SITE

We consider an electron wave function,

$$\psi_O(\vec{r}) = \mathcal{R}_l(r)Y_l^\tau(\Omega), \tag{A1}$$

at a site one centered at point O. Here the index τ stands for 0, (m,c), or (m,s) of real spherical harmonics,[32]

$$Y_l^{m,c}(\Theta,\phi) = C(l,m)P_l^m(\cos\Theta)\cos m\phi, \tag{A2a}$$

$$Y_l^{m,s}(\Theta,\phi) = C(l,m)P_l^m(\cos\Theta)\sin m\phi, \tag{A2b}$$

where P_l^m is the associated Legendre function, and

$$C(l,m) = \sqrt{\frac{(2l+1)(l-|m|)!}{2\pi(l+|m|)!}} \quad \text{if} \quad m \neq 0, \tag{A3a}$$

$$C(l,0) = \sqrt{\frac{(2l+1)}{4\pi}} \quad \text{if} \quad m = 0. \tag{A3b}$$

We write for expansion of this function in terms of spherical harmonics $Y_{l'}^{\tau'}(\Omega')$ given at a site two and centered at a different point O', see Fig. 8,

$$\psi_{O'}(\vec{r}') = \sum_{l',\tau'} \mathcal{R}_{l,l'}^{\tau'}(r')Y_{l'}^{\tau'}(\Omega'). \tag{A4}$$

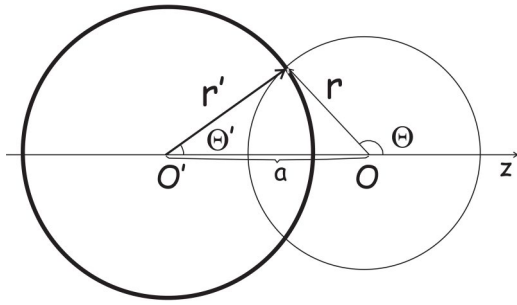The radial dependence $\mathcal{R}_{l,l'}^{\tau'}(r')$ can be written as

FIG. 8. The connection between r, r', Θ, Θ', and a. O and O' are the centers of expansion.

$$\mathcal{R}_{l,l'}^{\tau'}(r') = \int_0^{2\pi} d\phi' \int_0^\pi \sin\Theta' \, d\Theta' \, \psi_O(\vec{r}) Y_{l'}^{\tau'}(\Theta',\phi'),$$

(A5)

where $\vec{r}$ is an implicit function of (Θ',ϕ'), Fig. 8. It is convenient to consider r as a variable, while Θ and Θ' as functions of r,

$$\cos\Theta|_r = \frac{r'^2 - r^2 - a^2}{2ar}, \quad \cos\Theta'|_r = \frac{r'^2 - r^2 + a^2}{2ar'}. \quad \text{(A6)}$$

We notice that r changes from $\max(a-r', r'-a)$ till $a+r'$ (a is the distance between O and O', Fig. 8) while Θ' is changing from 0 till π. Substituting in Eq. (A5) Eq. (A1) for $\psi_O(\vec{r})$ and Eqs. (A2a) and (A2b) for the spherical harmonics, we arrive at

$$\mathcal{R}_{l,l'}^{m'}(r') = \delta_{m,m'} \frac{N(l,l',m)}{ar'}$$

$$\times \int_{r_{min}}^{r_{max}} P_l^m(\cos\Theta|_r) P_{l'}^m(\cos\Theta'|_r) \mathcal{R}_l(r) r \, dr.$$

(A7a)

Here $r_{min} = \max(a-r', r'-a)$ and $r_{max} = a+r'$, and

$$N(l,l',m) = k\pi C(l,m) C(l',m), \quad \text{(A7b)}$$

where $k=1$ if $m \neq 0$, and $k=2$ if $m=0$. Notice that the azimuthal integration ensures that $\tau' = \tau$ and the radial dependence $\mathcal{R}_{l'}^m(r')$, Eq. (A7a), is exactly the same for $\tau' = (m,c)$ and (m,s), provided that $\mathcal{R}_l(r)$ in Eq. (A1) stays the same for $\tau = (m,c)$ and (m,s), which is usually the case. In the present work the integration in Eq. (A7a) has been performed numerically.

We start with the coordinate wave function of the s state at the site O:

$$\psi_{A,s}(\vec{r}) = \mathcal{R}_s(r) Y_0^0, \quad \text{(A8)}$$

where $Y_0^0 = 1/\sqrt{4\pi}$. The expansion of the state at the site O' (first fullerene site, Fig. 1) reads as

$$\psi_{A,s}(\vec{r}') = \sum_{l=0}^{L_{max}} \mathcal{R}_{s,l}(r') Y_l^0(\Omega'), \quad \text{(A9)}$$

where the spherical harmonics Y_l^0 and the radial function $\mathcal{R}_{s,l}$ are written now for the radius vector $\vec{r}'$ of the fullerene site O'. In principle, the sum in Eq. (A9) runs over all values of

$l \geq 0$, in practice we limit it by $L_{max} = 6$. Analogously we treat the d states of the alkali atom. We start with the coordinate function

$$\psi_{A,d,\tau}(\vec{r}) = \mathcal{R}_d(r) Y_{l=2}^\tau \quad \text{(A10)}$$

at the site O, which becomes

$$\psi_{A,d,\tau}(\vec{r}') = \sum_{l=m}^{L_{max}} \mathcal{R}_{d,l}^m(r') Y_l^\tau(\Omega') \quad \text{(A11)}$$

at the fullerene site O'. Here $\tau = 0$, (m,c) or (m,s).

The procedure outlined in Eqs. (A8)–(A11) can be formalized in the following way. The state of the alkali atom is described by index $i_a = (k^a, s_z)$, Sec. III A, which include the spin $[u(s_z)]$ and orbital part $[k^a = 1$ for the s state or $k^a = 2$–6 for d states; $\tau = 0$, (m,c) and (m,s), $m=1,2]$. Expanding the orbital part of i_a at the fullerene site O', we introduce the states $i_{a,p}$, which in the following we call projected states. They have the same spin component $[u(s_z)]$ as the initial alkali state i_a, while the index p refers to different spherical harmonics on the right hand side of Eqs. (A9) and (A11). The corresponding radial functions are labeled as $\mathcal{R}_{i_a,p}(r')$. Thus, formally we can write

$$\langle \vec{r}|i_a\rangle_O = \sum_p \mathcal{R}_{i_a,p}(r')\langle \hat{n}'|i_{a,p}\rangle_{O'}. \quad \text{(A12)}$$

The same expansion can be introduced for the t_{1u} molecular orbitals. However, since for a general rotation $R(\omega)$ of the C_{60} molecule, the orbital functions $\psi_k' = R(\omega)\psi_k$ are expressed as linear combinations of all spherical harmonics $Y_{l=5}^\tau$, it is convenient to consider first all 11 orbital basis states (h states)

$$\langle \vec{r}|i^\tau\rangle = \mathcal{R}_t(r) Y_{l=5}^\tau(\Omega), \quad \text{(A13)}$$

where $\tau = 0$, (m,c), and (m,s) with $m=1$–5. These h states taken at a site O can be also expanded in terms of projected states (i_p^τ) at a site O',

$$\langle \vec{r}|i^\tau\rangle_O = \sum_p \mathcal{R}_{i^\tau,p}(r')\langle \hat{n}'|i_p^\tau\rangle_{O'}. \quad \text{(A14)}$$

The t_{1u} molecular orbitals are restored if we take the linear combinations of h states as in Eqs. (2.1a), (2.1b), and (2.1c).

APPENDIX B: SINGLE-ELECTRON OPERATORS

The effective potential of the alkali atom is defined as

$$U^a(r) = -\frac{Z}{r} + V_C(r) + V_{xc}(r). \quad \text{(B1)}$$

Here Z is the nuclear charge (in e), V_C is the Coulomb potential of the core electrons, and V_{xc} is the exchange-correlation part of the core electrons calculated in the local density approximation (LDA).

For the fullerene molecule as a core we consider all occupied states except the valence t_{1u} level (360 electrons). To describe their electron density we employ the expansion tabulated by Savin *et al.*[57] In this work we have used only the spherical symmetric component[58] $\rho_0(r)$ quoted in Table III of Ref. 57. Starting with $\rho_0(r)$, we have constructed the

effective potential $U^{C60}(r)$ comprising the potential of 60 carbon nuclei and the potential of the core electrons as in Eq. (B1). In the following we discuss the matrix elements which involve the effective potentials U^a and U^{C60}.

If an electron stays at the fullerene site, i.e., we consider one-electron transition $i_a \rightarrow j_a$, then the attraction to the effective potential $U^a(r)$ is found as

$$\langle i_a | U^a(\vec{r}) | j_a \rangle = \delta(i_a, j_a) \int dr r^2 \mathcal{R}_{i_a}(r) U^a(r) \mathcal{R}_{i_a}(r). \quad \text{(B2)}$$

To describe an electron transferred to the fullerene site we first introduce auxiliary 11 h states $|j^\tau\rangle$, Eq. (A13). We expand j^τ in terms of spherical harmonics at the alkali site and use notations j_p^τ for these states, Appendix A. The attraction to the alkali site then is found as

$$\langle i_a | U^a(\vec{r}) | j^\tau \rangle = \int dr \, r^2 \mathcal{R}_{i_a}(r) U^a(r) \mathcal{R}_{j^\tau, p}(r). \quad \text{(B3)}$$

Notice that in the latter expression there is no summation on p, because *only one state of the same angular symmetry* as i_a gives the contribution. This is a consequence of the fact that $U^a(r)$ has the spherical symmetry.

Analogously, we can find the attraction to the C_{60} molecule, i.e., the matrix elements of $\langle i^t | U^{C60}(\vec{r}) | j^t \rangle$ and $\langle i^t | U^{C60}(\vec{r}) | j_a \rangle$. The total attraction for a transferred electron is given by

$$\langle i^t | U^{attr}(\vec{r}) | j_a \rangle = \langle i^t | U^a(\vec{r}) | j_a \rangle + \langle i^t | U^{C60}(\vec{r}) | j_a \rangle. \quad \text{(B4)}$$

If an electron remains at the same site, we obtain

$$\langle i^t | U^{attr}(\vec{r}) | j^t \rangle = \langle i^t | U^a(\vec{r}) | j^t \rangle + \langle i^t | U^{C60}(\vec{r}) | j^t \rangle, \quad \text{(B5a)}$$

$$\langle i_a | U^{attr}(\vec{r}) | j_a \rangle = \langle i_a | U^a(\vec{r}) | j_a \rangle + \langle i_a | U^{C60}(\vec{r}) | j_a \rangle. \quad \text{(B5b)}$$

We now calculate $\langle i_a | U^{C60}(\vec{r}) | j_a \rangle$ and $\langle i^t | U^a(\vec{r}) | j^t \rangle$. We expand the states i_a and j_a, in terms of $i_{a,p}$ and $j_{a,p}$ of the fullerene site, and obtain

$$\langle i_a | U^{C60}(r) | j_a \rangle = \sum_p \int dr \, r^2 \mathcal{R}_{i_{a,p}}(r) U^{C60}(r) \mathcal{R}_{j_{a,p}}(r). \quad \text{(B6)}$$

Only one index p occurs because of the spherical symmetry of $U^{C60}(r)$. Analogously, one finds $\langle i^t | U^a(r) | j^t \rangle$.

From Eqs. (B2) and (B3) one can deduce the overlap matrix elements. For this we formally put $U^a = 1$ in Eqs. (B2) and (B3). Then from Eq. (B3) we find

$$s(i_a, j^\tau) = \langle i_a | j^\tau \rangle = \int dr \, r^2 \mathcal{R}_{i_a}(r) \mathcal{R}_{j^\tau, p}(r). \quad \text{(B7)}$$

To obtain the matrix elements of the kinetic energy we notice that only states with the same angular dependence Y_l^τ give nonzero elements, which can further be found as

$$K_{12} = \frac{1}{2} \int \frac{d\mathcal{R}_1(r)}{dr} \frac{d\mathcal{R}_2(r)}{dr} r^2 dr + \frac{1}{2} l(l+1) \int \mathcal{R}_1(r) \mathcal{R}_2(r) dr. \quad \text{(B8)}$$

Here $\mathcal{R}_1$ and $\mathcal{R}_2$ refer to the radial parts of the corresponding wave functions.

Finally, the repulsion energy V_{cc} between the core alkali site and the core fullerene site is calculated as follows. We expand the potential $U^{C60}(r)$ in terms of spherical harmonics on another site which is the alkali site as described in Appendix A. We need only the spherically symmetric component $U_{p0}^{C60}(r)$. Then the energy of the alkali nucleus in the potential U^{C60} is

$$U_1 = - U_{p0}^{C60}(r=0)Z. \quad \text{(B9a)}$$

The energy of the alkali core electrons in U^{C60} is

$$U_2 = \int dr \, r^2 \rho_0^a(r) U_{p0}^{C60}(r), \quad \text{(B9b)}$$

where $\rho_0^a(r)$ is the density of the alkali core electrons. The total repulsion energy is $U^{rep} = U_1 + U_2$, and the matrix elements are given by

$$\langle I | U^{rep} | J \rangle = U^{rep} \langle I | J \rangle. \quad \text{(B10)}$$

[1] H. A. Kramers, Physics (N.Y.) **1**, 182 (1934).
[2] P. W. Anderson, Phys. Rev. **79**, 350 (1950).
[3] For a review, see P. Fulde, *Electron Correlations in Molecules and Solids* (Springer, Heidelberg, 1995).
[4] D. Jérome, Science **252**, 1509 (1991).
[5] P. W. Anderson, Science **235**, 1196 (1987).
[6] For a review, see J. S. Miller and A. J. Epstein, Angew. Chem., Int. Ed. Engl. **33**, 385 (1994); MRS Bull. **25**, 11 (2000).
[7] O. Gunnarsson, Rev. Mod. Phys. **69**, 575 (1997).
[8] M. S. Dresselhaus, J. Dresselhaus, and P. C. Eklund, *Science of Fullerenes and Carbon Nanotubes* (Academic, New York, 1995).
[9] K. Tanigaki and K. Prassides, J. Mater. Chem. **5**, 1515 (1995).
[10] L. Forró and L. Mihály, Rep. Prog. Phys. **64**, 649 (2001).
[11] R. C. Haddon, L. F. Schneemeyer, J. V. Waszczak *et al.*, Nature (London) **350**, 320 (1991); A. F. Hebard, M. J. Rosseinsky, R. C. Haddon, D. W. Murphy, S. H. Glarum, T. T. M. Palstra, A. P. Ramirez, and A. R. Kortan, *ibid.* **350**, 600 (1991); M. J. Rosseinsky, A. P. Ramirez, S. H. Glarum *et al.*, Phys. Rev. Lett. **66**, 2830 (1991); K. Holczer, O. Klein, S. M. Huang, R. B. Kaner, K. J. Fu, R. L. Whetten, and F. Diederich, Science **252**, 1154 (1991).
[12] J. Winter and H. Kuzmany, Solid State Commun. **84**, 935 (1992); Q. Zhu, O. Zhou, J. E. Fischer, A. R. McGhie, W. J. Romanow, R. M. Strongin, M. A. Cichy, and A. B. Smith, Phys. Rev. B **47**, 13948 (1993).
[13] S. Pekker, L. Forró, L. Mihály, and A. Janossy, Solid State Commun. **90**, 349 (1994).
[14] P. W. Stephens, G. Bortel, G. Faigel, M. Tegze, A. Jánossy, S. Pekker, G. Oszlányi, and L. Forró, Nature (London) **370**, 636 (1994).
[15] R. Tycko, G. Dabbagh, D. W. Murphy, Q. Zhu, and J. E. Fischer, Phys. Rev. B **48**, 9097 (1993).
[16] F. Bommeli, L. Degiorgi, P. Wachter, Ö. Legeza, A. Jánossy, G. Oszlanyi, O. Chauvet, and L. Forro, Phys. Rev. B **51**, 14794 (1995).
[17] P. Launois, R. Moret, J. Hone, and A. Zettl, Phys. Rev. Lett. **81**, 4420 (1998).
[18] S. Rouzière, S. Margadonna, K. Prassides, and A. N. Fitch, Europhys. Lett. **51**, 314 (2000).
[19] C. Coulon, A. Pénicaud, R. Clérac, R. Moret, P. Launois, and J. Hone, Phys. Rev. Lett. **86**, 4346 (2001); B. Verberck, A. V. Nikolaev, and K. H. Michel, Phys. Rev. B **66**, 165425 (2002).
[20] O. Chauvet, G. Oszlanyi, L. Forro, P. W. Stephens, M. Tegze, G. Faigel, and A. Janossy, Phys. Rev. Lett. **72**, 2721 (1994).
[21] K. H. Michel and A. V. Nikolaev, Phys. Rev. Lett. **85**, 3197 (2000); B. Verberck, K. H. Michel, and A. V. Nikolaev, J. Chem. Phys. **116**, 10462

(2002).

[22] T. Yildirim, L. Barbedette, J. E. Fischer, C. L. Lin, J. Robert, P. Petit, and T. T. M. Palstra, Phys. Rev. Lett. **77**, 167 (1996).

[23] S. C. Erwin, G. V. Krishna, and E. J. Mele, Phys. Rev. B **51**, 7345 (1995).

[24] A. V. Nikolaev and K. H. Michel, J. Chem. Phys. **117**, 4761 (2002).

[25] M. Luders, A. Bordon, N. Manini, A. Dal Corso, M. Fabrizio, and E. Tosatti, Philos. Mag. B **82**, 1611 (2002).

[26] E. U. Condon and G. H. Shortley, *The Theory of Atomic Spectra* (Cambridge University Press, Cambridge, 1967).

[27] W. Heitler and F. London, Z. Phys. **44**, 455 (1927); L. Pauling, *The Nature of the Chemical Bond and the Structure of Molecules and Crystals*, 3rd ed. (Cornell University Press, Ithaca, NY, 1960).

[28] A. V. Nikolaev, K. Prassides, and K. H. Michel, J. Chem. Phys. **108**, 4912 (1998).

[29] R. C. Haddon, L. E. Brus, and K. Raghavachari, Chem. Phys. Lett. **125**, 459 (1986); R. C. Haddon, Science **261**, 1545 (1993).

[30] N. V. Cohan, Proc. Cambridge Philos. Soc. **54**, 28 (1958).

[31] E. Tosatti, N. Manini, and O. Gunnarsson, Phys. Rev. B **54**, 17184 (1996).

[32] C. J. Bradley and A. P. Cracknell, *The Mathematical Theory of Symmetry in Solids* (Clarendon, Oxford, 1972).

[33] W. I. F. David, R. M. Ibberson, J. C. Matthewman, K. Prassides, T. J. S. Dennis, J. P. Hare, H. W. Kroto, and D. R. M. Walton, Nature (London) **353**, 147 (1991).

[34] M. Tinkham, *Group Theory and Quantum Mechanics* (McGraw-Hill, New York, 1964).

[35] J. Slater and G. F. Koster, Phys. Rev. **94**, 1498 (1954).

[36] P. Rudolf, M. S. Golden, and P. A. Brühwiler, J. Electron Spectrosc. Relat. Phenom. **100**, 409 (1999).

[37] D. M. Poirier, C. G. Olson, and J. H. Weaver, Phys. Rev. B **52**, R11662 (1995); P. J. Benning, F. Stepniak, and J. H. Weaver, Phys. Rev. B **48**, 9086 (1993).

[38] W. Andreoni, P. Giannozzi, and M. Parrinello, Phys. Rev. B **51**, 2087 (1995).

[39] K. Jorissen and D. Lamoen, FLAPW calculations (Wien code), unpublished.

[40] R. F. W. Bader, Acc. Chem. Res. **18**, 9 (1985).

[41] C. Hartwigsen, W. Witschel, and E. Spohr, Phys. Rev. B **55**, 4953 (1997).

[42] C. P. Slichter, *Principles of Magnetic Resonance*, 3rd ed. (Springer, Berlin, 1990).

[43] A. V. Nikolaev and K. H. Michel, Solid State Commun. **117**, 739 (2001).

[44] B. Verberck, V. N. Popov, A. V. Nikolaev, and D. Lamoen, J. Chem. Phys. **121**, 321 (2004).

[45] B. Simovič, D. Jérome, F. Rachdi, G. Baumgartner, and L. Forró, Phys. Rev. Lett. **82**, 2298 (1999).

[46] B. Simovič, D. Jérome, and L. Forró, Phys. Rev. B **63**, 125410 (2001).

[47] M. Kosaka, K. Tanigaki, T. Tanaka, T. Atake, A. Lappas, and K. Prassides, Phys. Rev. B **51**, 12018 (1995); A. Lappas, M. Kosaka, K. Tanigaki, and K. Prassides, J. Am. Chem. Soc. **117**, 7560 (1995).

[48] R. Sachidanandam and A. B. Harris, Phys. Rev. Lett. **67**, 1467 (1991); A. B. Harris and R. Sachidanandam, Phys. Rev. B **46**, 4944 (1992).

[49] For a review on structure and dynamics of crystallic C_{60}, see: J. D. Axe, S. C. Moss, and D. A. Neumann, *Solid State Physics*, edited by H. E. Ehrenreich and F. Spaepen (Academic, New York, 1994), Vol. 48, p. 149.

[50] W. I. F. David, R. M. Ibberson, T. J. S. Dennis, J. P. Hare, and K. Prassides, Europhys. Lett. **18**, 219 (1992).

[51] V. Brouet, H. Alloul, F. Quéré, G. Baumgartner, and L. Forró, Phys. Rev. Lett. **82**, 2131 (1999).

[52] V. Brouet, H. Alloul, and L. Forró, Phys. Rev. B **66**, 155123 (2002).

[53] F. Keffer and T. Oguchi, Phys. Rev. **115**, 1428 (1959).

[54] R. McWeeny, *Methods of Molecular Quantum Mechanics* (Academic, London, 1992).

[55] V. S. Mironov, J. Phys.: Condens. Matter **8**, 10551 (1996).

[56] E. Dagotto, Rev. Mod. Phys. **66**, 763 (1994).

[57] S. Savin, A. B. Harris, and T. Yildirim, Phys. Rev. B **55**, 14182 (1997).

[58] In Ref. 57 the electron density $\rho_0(r)$ is normalized to 240 electrons. The other 120 electrons simply compensate the charge of 60 carbon nuclei.